JACS
JOURNAL OF THE AMERICAN CHEMICAL SOCIETY

ARTICLE

pubs.acs.org/JACS

Molecular Accordion: Vapoluminescence and Molecular Flexibility in the Orange and Green Luminescent Crystals of the Dimer, $Au_2(\mu$-bis-(diphenylphosphino)ethane$)_2Br_2$

Sang Ho Lim, Marilyn M. Olmstead, and Alan L. Balch*

Department of Chemistry, University of California, Davis, California 95616, United States

Supporting Information

ABSTRACT: Solutions containing the components Au^+, dppe (dppe is bis(diphenylphosphino)ethane), and Br^- in a 1:1:1 ratio can produce three different types of crystals: type A, orange luminescent solvates of the dimer $Au_2(dppe)_2Br_2$ ($Au_2(\mu$-dppe$)_2Br_2\cdot 2(OSMe_2)$, $Au_2(\mu$-dppe$)_2Br_2\cdot 2(OCMe_2)$, $Au_2(\mu$-dppe$)_2Br_2\cdot 2(CH_2Cl_2)$, $Au_2(\mu$-dppe$)_2Br_2\cdot 2(HC(O)NMe_2)$); type B, green luminescent solvates of the same dimer ($Au_2(\mu$-dppe$)_2Br_2\cdot$(NCMe) and $Au_2(\mu$-dppe$)_2Br_2\cdot 0.5(C_4H_{10}O)$); and type C, orange luminescent solvates of a polymer ($\{Au(\mu$-dppe$)Br\}_n\cdot 0.5(C_4H_{10}O)$ and $\{Au(\mu$-dppe$)Br\}_n\cdot(CH_2Cl_2)$). Some crystals of types A are solvoluminescent. Exposure of type A crystals of $Au_2(\mu$-dppe$)_2Br_2\cdot 2(OCMe_2)$ or $Au_2(\mu$-dppe$)_2Br_2\cdot 2(CH_2Cl_2)$ to air or vacuum results in the loss of the orange luminescence and the formation of new green luminescent crystals. Subsequent exposure of these crystals to acetone or dichloromethane vapor results in the reformation of crystals of type A. The dimeric complexes in crystals of types A and B are all centrosymmetric and share a common ring conformation. Within these dimers, the coordination geometry of each gold center is planar with a P_2Br donor set. In other respects, the $Au_2(\mu$-dppe$)_2Br_2$ molecule is remarkably flexible and behaves as a molecular accordion, whose dimensions depend upon the solvate content of a particular crystalline phase. In particular, the dimer $Au_2(\mu$-dppe$)_2Br_2$ is able to accommodate Au···Au separations that range from 3.8479(3) to 3.0943(2) Å, and these variations along with alterations in the Au−Br distances and in the P−Au−P angles are the likely causes of the differences in the luminescence properties of these crystals.

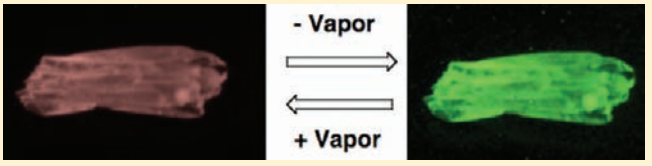

INTRODUCTION

Vapoluminescent and vapochromic transition metal complexes change their luminescence or color in response to exposure to vapors of volatile organic compounds. Consequently, they can be developed into sensors for various volatile molecules.[1−3] For metal complexes with low coordination numbers, the formation of metal−metal interactions (metallophillic attractions)[4,5] produces suitable chromophores that can exhibit vapochromic and/or vapoluminescent behavior. These vapoluminescent and vapochromic compounds generally function by absorbing the volatile molecule, which can interact with the chromophor or lumophor in a variety of ways. In many cases, the volatile molecule becomes coordinated to a metal ion as happens in the linear polymeric chain complex, $\{Tl[Au(C_6Cl_5)_2]\}_n$, where various volatile Lewis bases bind to the thallium ions and alter the thallium−gold interactions.[6] Other interesting examples that also entail metal ion coordination of the volatile substance include a trinuclear Cu_2Au complex,[7] a polymeric Au−Ag compound,[8] and simple copper(I) cyanide.[9] Platinum chain complexes of the type $[Pt(CNR)_4]$-$[Pt(CN)_4]$ show particularly dramatic vapochromic and vapoluminescent effects, which result from alterations in the Pt···Pt separations that occur when volatile molecules are incorporated into these solids.[10−12] Hydrogen bonding between the cyanide ligands and the adsorbed molecules also can play an important role in causing the vapochromic and vapoluminescent changes.[13]

The closed-shell, diamagnetic d^{10} gold(I) ion produces an interesting array of luminescent complexes with varied properties.[14,15] Mononuclear, two-coordinate gold(I) complexes are generally colorless and are usually nonluminescent when the individual gold(I) centers are isolated from one another. However, two coordinate gold(I) complexes can become luminescent when two or more gold(I) centers are placed in close proximity. Aurophilic interactions, attractive interactions between gold centers caused by a combination of relativistic effects and correlation effects,[16] facilitate the formation of aggregates of two-coordinate gold(I) complexes, and these aurophilic interactions can be promoted through the use of suitable bridging ligands. The distance between gold atoms in metallic gold is 2.89 Å, while the Au···Au separation expected from the van der Waals radius is about 3.6 Å.[17] When the Au···Au separation is less than 3.6 Å, some degree of aurophilic interaction may be expected, and numerous gold(I) complexes display structural evidence of aurophilic attractions.[2,3,18]

Despite the abundance of aurophilic interactions that connect two-coordinate gold(I) complexes, aurophilic interactions between three-coordinate gold(I) complexes are rare.[19] The cases where such an interaction is found involve the complexes shown in

Received: March 24, 2011
Published: May 26, 2011

dx.doi.org/10.1021/ja2026807 | J. Am. Chem. Soc. 2011, 133, 10229–10238

Scheme 1 where two or three small-bite ligands bridge the two gold(I) centers and enforce their proximity. Thus, in $[Au_2(\mu\text{-dmpm})_3](BF_4)_2$ (where dmpm is bis(dimethylphosphino)methane, E = PMe_2, B = CH_2) the Au···Au distances are 3.040(1) and 3.050(1) Å for the two different molecules in the asymmetric unit.[20] Similarly, in $[Au_2\{(Ph_2Sb)_2O\}_3](ClO_4)_2$ (E = $SbPh_2$, B = O) the Au···Au distance is 3.0320(4) Å,[21] and in $Au_2(\mu\text{-dppm})_2Br_2$ (E = PPh_2, B = CH_2, X = Br) the Au···Au distance is 3.015(1) Å.[22] Other cases of aurophilic interactions between possibly three-coordinate gold centers involve the accordion-like structure shown in Scheme 1 with two bridging small-bite phosphine ligands and terminal chloride ligands.[23−25] However, in these cases the Au−Cl distances are quite long (greater than 2.7 Å).

Unlike monomeric, two-coordinate gold(I) complexes, mononuclear three-coordinate gold(I) complexes are frequently luminescent both in the solid state and in solution.[26−28] For these three-coordinate complexes, the excitation process is generally attributed to a transition from the filled, in-plane $d_{x^2-y^2}$,d_{xy} orbitals on gold to its empty p_z orbital. Recent computational and experimental studies have analyzed the structural changes that are found in the excited states of these three-coordinate complexes. In particular, distortions from nominally trigonal ground states to and beyond a T-shape have been proposed based upon computational studies of complexes of the types $[Au(PR_3)_3]^+$ and $Au(PR_3)_2X$ (X = halide).[29,30] In contrast, photocrystallographic studies of $Au(PR_3)_2Cl\cdot CHCl_3$ and $Au(PR_3)_3Cl$ showed bond shortening in the excited state, while a similar study of the second polymorph of $Au(PR_3)_2Cl$ revealed little change between the structures of the crystals with and without photoexcitation.[31−33]

Here we report the remarkable structural flexibility and vapoluminescent properties of three-coordinate gold(I), accordion-like complexes (see II in Scheme 1) formed with dppe (dppe is bis(diphenylphosphino)ethane) and bromide ion as ligands.

Scheme 1. Binuclear Gold(I) Complexes

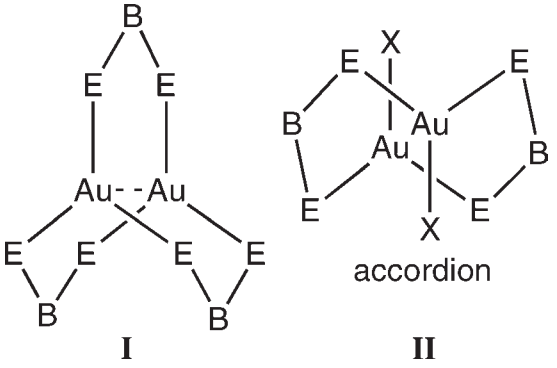

RESULTS AND DISCUSSION

Preparation and Crystal Growth. Simple mixing of the labile complex (tht)AuBr with dppe in either dichloromethane or acetone results in the formation of a colorless product with a green luminescence that can be crystallized from a variety of solvents to produce three distinct types of colorless crystals, each of which is a solvate. Colorless crystals that produce an orange emission when irradiated with a UV lamp (type A) are obtained from dimethyl sulfoxide, acetone, dichloromethane, or *N*,*N*-dimethylformamide and contain molecules of the dimer, $Au_2(\mu\text{-dppe})_2Br_2$, along with those of the respective solvent. However, colorless crystals that produce green emission (type B) are obtained as acetonitrile or diethyl ether solvates. These

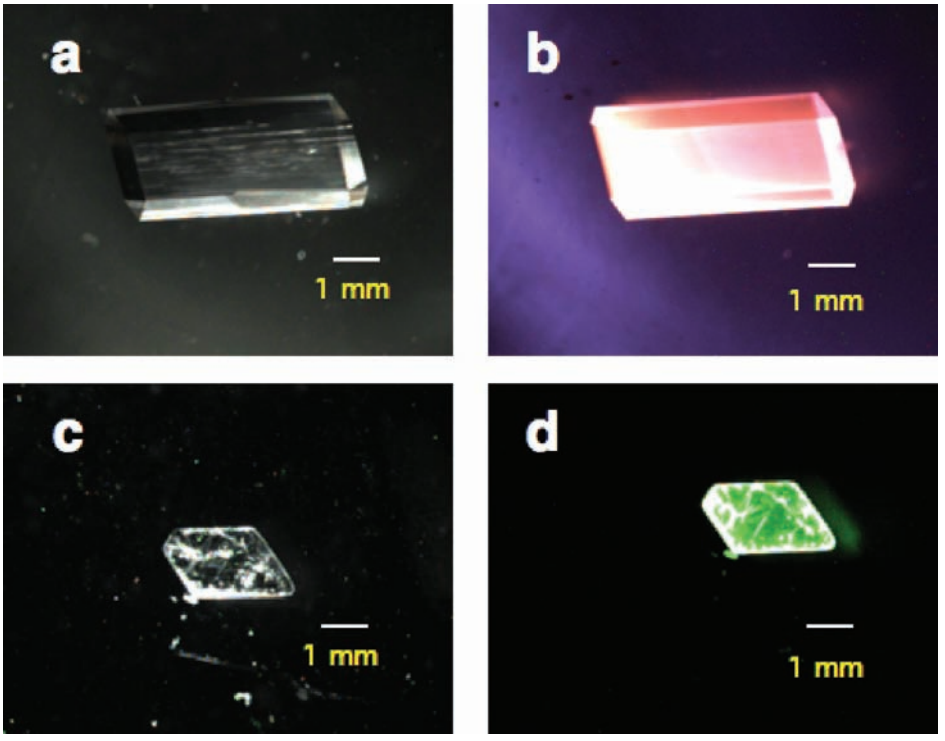

Figure 1. Photographs of a type A crystal of $Au_2(\mu\text{-dppe})_2Br_2\cdot 2(HC(O)NMe_2)$ under (a) ambient and (b) UV light and of a type B crystal of $Au_2(\mu\text{-dppe})_2Br_2\cdot(NCMe)$ under (c) ambient and (d) UV light.

Table 1. Crystal Data and Data Collection Parameters

	$Au_2(\mu\text{-dppe})_2Br_2 \cdot 2(OSMe_2)$	$Au_2(\mu\text{-dppe})_2Br_2 \cdot 2(OCMe_2)$	$Au_2(\mu\text{-dppe})_2Br_2 \cdot 2CH_2Cl_2$	$Au_2(\mu\text{-dppe})_2Br_2 \cdot 2(HC(O)NMe_2)$
formula	$C_{52}H_{48}Au_2Br_2P_4 \cdot 2(C_2H_6OS)$	$C_{52}H_{48}Au_2Br_2P_4 \cdot 2(C_3H_6O)$	$C_{52}H_{48}Au_2Br_2P_4 \cdot 2(CH_2Cl_2)$	$C_{52}H_{48}Au_2Br_2P_4 \cdot 2(C_3H_7NO)$
	type A	type A	type A	type A
formula weight	1506.79	1466.69	1520.38	1496.73
T, K	90(2)	90(2)	90(2)	90(2)
color and habit	colorless block	colorless block	colorless block	colorless parallelepiped
crystal system	monoclinic	monoclinic	monoclinic	triclinic
space group	$P2_1/c$	$P2_1/c$	$P2_1/c$	$P\bar{1}$
a, Å	10.6725(4)	10.776(2)	10.7883(4)	11.0206(10)
b, Å	23.1389(9)	22.739(4)	22.4579(8)	11.6968(11)
c, Å	11.7127(5)	11.738(2)	11.6966(4)	12.2211(11)
α, deg	90	90	90	103.357(2)
β, deg	106.416(4)	106.848(3)	108.544(4)	101.085(2)
γ, deg	90	90	90	109.337(2)
V, Å^3	2774.54(19)	2752.8(8)	2686.75(17)	1382.9(2)
Z	2	2	2	1
d_{calcd}, g·cm^{-3}	1.804	1.769	1.879	1.797
μ, mm^{-1}	6.953	6.932	7.295	6.902
unique data	6391	8241	6165	8277
restraints	7	0	4	0
params.	312	309	297	318
R1[a]	0.0264	0.0206	0.022	0.0210
wR2[b]	0.0555	0.0444	0.055	0.0488
	$Au_2(\mu\text{-dppe})_2Br_2 \cdot (NCMe)$	$Au_2(\mu\text{-dppe})_2Br_2 \cdot 0.5(C_4H_{10}O)$	$\{Au(\mu\text{-dppe})Br\}_n \cdot 0.5(C_4H_{10}O)$	$\{Au(\mu\text{-dppe})Br\}_n \cdot (CH_2Cl_2)$
formula	$C_{52}H_{48}Au_2Br_2P_4 \cdot (C_2H_3N)$	$C_{52}H_{48}Au_2Br_2P_4 \cdot 0.5(C_4H_{10}O)$	$C_{26}H_{24}AuBrP \cdot 0.5(C_4H_{10}O)$	$C_{26}H_{24}AuBrP \cdot (CH_2Cl_2)$
	type B	type B	type C	type C
formula weight	1391.59	1424.64	713.32	760.19
T, K	90(2)	90(2)	90(2)	90(2)
color and habit	colorless plate	colorless irregular block	colorless irregular block	colorless block
crystal system	triclinic	triclinic	monoclinic	triclinic
space group	$P\bar{1}$	$P\bar{1}$	$C2/c$	$P\bar{1}$
a, Å	11.8336(4)	11.7530(3)	26.0742(13)	9.1275(4)
b, Å	14.4702(5)	14.4241(3)	9.0076(5)	12.0795(5)
c, Å	15.2751(5)	15.4879(3)	24.0854(12)	13.7259(6)
α, deg	77.090(2)	76.550(3)	90	67.432(3)
β, deg	78.172(2)	77.600(3)	111.493(5)	71.848(3)
γ, deg	80.294(3)	79.600(3)	90	83.965(4)
V, Å^3	2474.62(15)	2470.35(9)	5263.5(5)	1327.75(10)
Z	2	2	4	2
d_{calcd}, g·cm^{-3}	1.868	1.865	1.798	1.901
μ, mm^{-1}	7.703	7.716	7.246	7.381
unique data	11403	14398	6079	8089
restraints	0	6	0	0
params.	565	577	312	298
R1[a]	0.017	0.023	0.031	0.032
wR2[b]	0.041	0.046	0.0713	0.0832

[a] For data with $I > 2\sigma I$, $R1 = \Sigma||Fo| - Fc||/\Sigma|Fo|$. [b] For all data. $wR2 = (\Sigma[w(Fo^2 - Fc^2)^2])/(\Sigma[w(Fo^2)^2])^{1/2}$.

crystals also contain the dimeric $Au_2(\mu\text{-dppe})_2Br_2$. Figure 1 shows photographs of examples of type A ($Au_2(\mu\text{-dppe})_2Br_2 \cdot 2(HC(O)NMe_2)$) and type B ($Au_2(\mu\text{-dppe})_2Br_2 \cdot (NCMe)$) crystals under ambient light and under UV irradiation. Finally, colorless, orange luminescent crystals of the polymer $\{Au(\mu\text{-dppe})Br\}_n$ (type C) have been obtained as concomitant polymorphs or pseudopolymorphs incorporating either dichloromethane or diethyl ether as described below.

The type A crystals of $Au_2(\mu\text{-dppe})_2Br_2 \cdot 2(OSMe_2)$ and $Au_2(\mu\text{-dppe})_2Br_2 \cdot 2(HC(O)NMe_2)$ are readily obtained as the only type of crystal produced when the initial colorless product is dissolved in the appropriate solvent and the solution is allowed to

Table 2. Selected Bond Distances (Å) and Angles (deg) for Gold Complexes

bond distances (Å)	$Au_2(\mu\text{-dppe})_2Br_2\cdot 2(OSMe_2)$	$Au_2(\mu\text{-dppe})_2Br_2\cdot 2(OCMe_2)$	$Au_2(\mu\text{-dppe})_2Br_2\cdot 2(CH_2Cl_2)$	$Au_2(\mu\text{-dppe})_2Br_2\cdot 2(HC(O)NMe_2)$
	type A	type A	type A	type A
Au1···Au1A	3.8479(3)	3.7339(9)	3.5676(3)	3.5142(3)
Au1−Br1	2.8292(5)	2.8226(4)	2.8034(4)	2.8848(3)
Au1−P1	2.3097(10)	2.3051(6)	2.3060(9)	2.3041(6)
Au1−P2	2.3050(10)	2.3109(6)	2.3096(8)	2.3032(6)
bond angles (deg)				
P1···Au1···P2	156.21(4)	155.797(19)	154.19(3)	157.80(2)
P1···Au1···Br1	103.04(3)	101.824(18)	102.11(2)	96.582(16)
P2···Au1···Br1	100.60(3)	102.356(19)	103.63(2)	105.099(16)
Σ angles about Au1	359.85	359.977	359.93	359.48

bond distances (Å)	$Au_2(\mu\text{-dppe})_2Br_2\cdot(NCMe)$	$Au_2(\mu\text{-dppe})_2Br_2\cdot(NCMe)$	$Au_2(\mu\text{-dppe})_2Br_2\cdot 0.5(C_4H_{10}O)$	$Au_2(\mu\text{-dppe})_2Br_2\cdot 0.5(C_4H_{10}O)$
	site A	site B	site A	site B
	type B	type B	type B	type B
Au1···Au1A	3.31740(19)	3.09841(18)	3.3249(2)	3.0943(2)
Au1−Br1	2.7247(3)	2.7115(11)	2.7374(3)	2.7127(3)
Au1−P1	2.3033(6)	2.2995(6)	2.3085(7)	2.3019(7)
Au1−P2	2.3126(6)	2.3205(6)	2.3154(7)	2.3152(7)
bond angles (deg)				
P1···Au1···P2	145.10(2)	139.87(2)	146.69(2)	141.48(2)
P1···Au1···Br1	110.442(15)	114.328(15)	108.721(17)	112.073(18)
P2···Au1···Br1	104.266(15)	104.749(15)	104.443(18)	105.706(18)
Σ angles about Au1	359.81	358.95	359.85	359.25

bond distances (Å)	$\{Au(\mu\text{-dppe})Br\}_n\cdot 0.5(C_4H_{10}O)$	$\{Au(\mu\text{-dppe})Br\}_n\cdot(CH_2Cl_2)$
	type C	type C
Au1···Au1A	7.1529(7) intra	7.3645(4) intra
	9.0082(7) inter	8.3827(7) inter
Au1−Br1	2.7894(5)	2.8166(4)
Au1−P1	2.3118(13)	2.3123(10)
Au1−P2	2.3095(13)	2.3104(10)
bond angles (deg)		
P1···Au1···P2	150.67(4)	153.36(3)
P1···Au1···Br1	108.41(3)	98.74(2)
P2···Au1···Br1	100.86(3)	107.78(2)
Σ angles about Au1	359.94	359.88

evaporate. Likewise, crystals of $Au_2(\mu\text{-dppe})_2Br_2\cdot(NCMe)$ of type B are formed when an acetonitrile solution of the initial product is allowed to evaporate. When crystals are grown by layering diethyl ether over a dichloromethane solution of the initial colorless product, crystals of $Au_2(\mu\text{-dppe})_2Br_2\cdot 2(CH_2Cl_2)$ of type A develop in the lower region of the tube where the concentration of dichloromethane is high, while crystals of $\{Au(\mu\text{-dppe})Br\}_n\cdot(CH_2Cl_2)$ of type C grow in the upper portion of the tube in the diethyl ether-rich region. The situation for crystal growth involving layering diethyl ether over an acetone solution of the initial product is even more complex. Type A crystals of the orange glowing acetone solvate, $Au_2(\mu\text{-dppe})_2Br_2\cdot 2(OCMe_2)$, grow in the lower, acetone-rich portion of the tube, while type C crystals of the orange glowing diethyl ether solvate, $\{Au(\mu\text{-dppe})Br\}_n\cdot 0.5(C_4H_{10}O)$, grow in the diethyl ether-rich region in the upper part of the tube. Additionally, in some tubes, but not in all, there is a region in the upper portion in which type B, green glowing crystals of $Au_2(\mu\text{-dppe})_2Br_2\cdot 0.5(C_4H_{10}O)$ grow.

Although we have developed procedures to crystallize dimeric $Au_2(\mu\text{-dppe})_2Br_2$ and polymeric $\{Au(\mu\text{-dppe})Br\}_n$ in several different forms, we have not attempted to directly study the species present in solution. The ability to form both $Au_2(\mu\text{-dppe})_2Br_2$ and $\{Au(\mu\text{-dppe})Br\}_n$ from a single mixture of solvents certainly indicates that these complexes are quite labile in solution. An earlier study of related complexes by ^{31}P NMR spectroscopy has revealed the presence of several unidentified compounds along with $[Au(dppe)_2]^{2+}$ in a solution containing a 1:1:1 ratio of Au^+, dppe, and Cl^-.[34]

dx.doi.org/10.1021/ja2026807 |J. Am. Chem. Soc. 2011, 133, 10229–10238

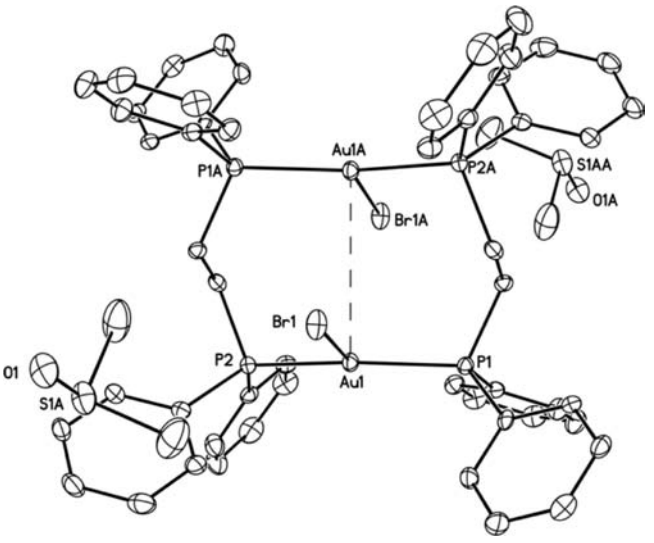

Figure 2. Drawing of the structure of $Au_2(\mu\text{-dppe})_2Br_2\cdot 2OSMe_2$, a representative crystal of type A. Thermal ellipsoids are shown at the 50% probability level.

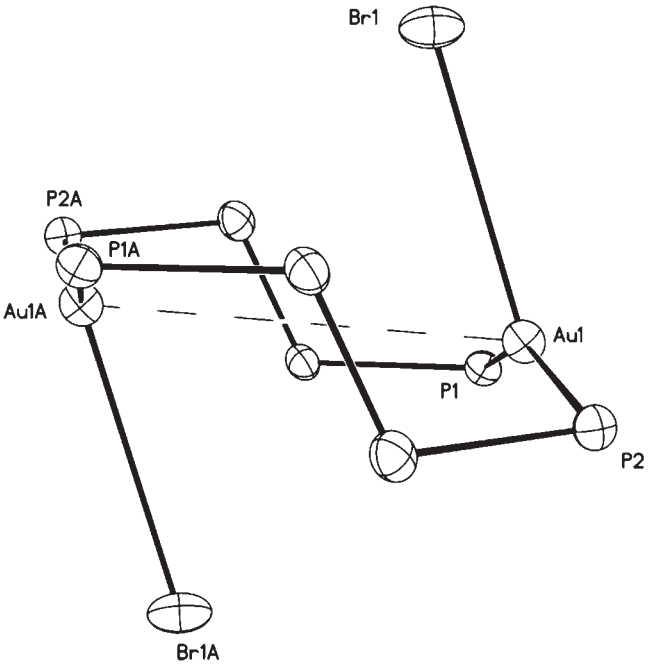

Figure 3. View of the ten-membered ring in $Au_2(\mu\text{-dppe})_2Br_2\cdot 2(OSMe_2)$. Thermal ellipsoids are shown at the 50% probability level. For clarity, the phenyl rings and the hydrogen atoms are omitted.

Structures of the Orange Luminescent Type A Crystals of $Au_2(\mu\text{-dppe})_2Br_2$. Crystal data for all complexes considered here are given in Table 1. Selected bond distances and angles are presented in Table 2. The structure of a representative example of a type A crystal, $Au_2(\mu\text{-dppe})_2Br_2\cdot 2(OSMe_2)$, is shown in Figure 2. The dimeric $Au_2(\mu\text{-dppe})_2Br_2$ molecule packs about a center of symmetry so that one-half of the dimer resides in the asymmetric unit. The gold centers are three-coordinate with bonds to two phosphorus atoms of two different bridging ligands and to the bromide ligand. Figure 3 shows a drawing of the ten-membered ring at the core of the dimer. Despite the fact that dimethyl sulfoxide is a good ligand, there is no bonding between it and the gold center. Indeed, it appears that the dimethyl sulfoxide molecule is merely filling space in the crystal.

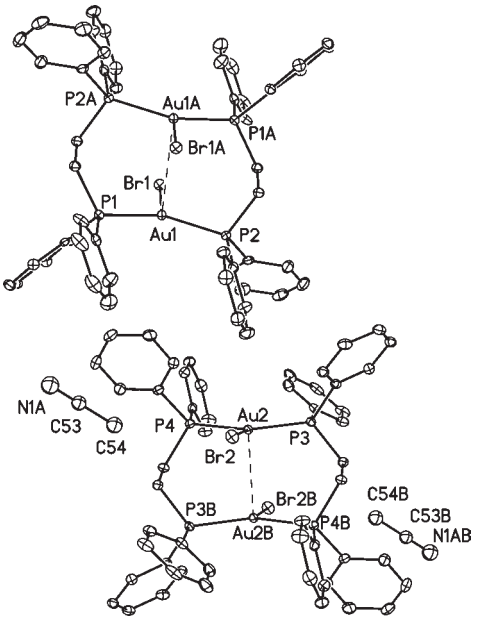

Figure 4. Drawing of the structure of $Au_2(\mu\text{-dppe})_2Br_2\cdot(CH_3CN)$, a representative crystal of type B. Thermal ellipsoids are shown at the 50% probability level. Hydrogen atoms are not shown for clarity.

The other crystals of type A have similar structural features. Indeed $Au_2(\mu\text{-dppe})_2Br_2\cdot 2(OSMe_2)$, $Au_2(\mu\text{-dppe})_2Br_2\cdot 2(OCMe_2)$, and $Au_2(\mu\text{-dppe})_2Br_2\cdot 2(CH_2Cl_2)$ are isostructural, while $Au_2(\mu\text{-dppe})_2Br_2\cdot 2(HC(O)NMe_2)$ crystallizes differently. In each case, the basic structures of the dimeric gold complex are similar, and there are no interactions of the solvate molecules with the three-coordinate gold centers. In all four structures, the ten-membered ring within the dimer has the conformation shown in Figure 3. The most noticeable difference in the structures is found in the separation between the gold centers, which range from 3.8479(3)Å in $Au_2(\mu\text{-dppe})_2Br_2\cdot 2(OSMe_2)$ to 3.5142(3) Å in $Au_2(\mu\text{-dppe})_2Br_2\cdot 2(HC(O)NMe_2)$.

Structures of the Green Luminescent Type B Crystals: $Au_2(\mu\text{-dppe})_2Br_2\cdot(NCMe)$ and $Au_2(\mu\text{-dppe})_2Br_2\cdot 0.5(C_4H_{10}O)$. Crystals of $Au_2(\mu\text{-dppe})_2Br_2\cdot(NCMe)$ and $Au_2(\mu\text{-dppe})_2Br_2\cdot 0.5(C_4H_{10}O)$ are isostructural as seen from the data in Table 1. A drawing of the molecular components in $Au_2(\mu\text{-dppe})_2Br_2\cdot(NCMe)$ is shown in Figure 4. There are two separate half molecules of the dimeric gold complex and an acetonitrile molecule in the asymmetric unit. As is the case in crystals of type A, the dimeric molecules in the type 2 crystals pack about crystallographic centers of symmetry. In each of the two solvates, the two gold dimers have structures remarkably similar to those found in the type A crystals. Each dimer has the same conformation for the ten-membered ring at its core as shown in Figure 3. However, in each type B crystal the Au···Au separations in the two different dimers differ significantly. In the acetonitrile solvate the two Au···Au distances are 3.31740(19) and 3.09841(18) Å, while in the diethyl ether solvate those distances are 3.3249(2) and 3.0943(2) Å. Additionally, these Au···Au distances are all considerably shorter than the corresponding Au···Au distances in the type A crystals, which range from 3.8479(3) to 3.5142(3) Å.

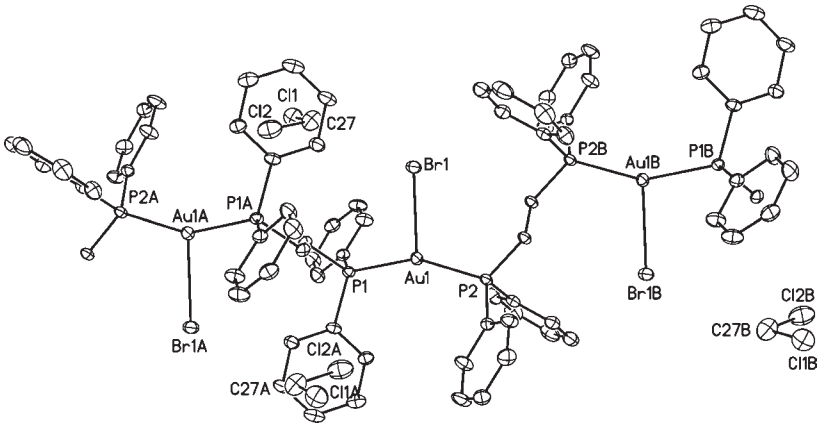

Figure 5. Drawing of a portion of the polymeric chain in $\{Au(\mu\text{-dppe})Br\}_n \cdot (CH_2Cl_2)$, a representative crystal of type C. Thermal ellipsoids are shown at the 50% probability level. Hydrogen atoms are not shown for clarity.

Table 3. Selected Bond Distances (Å) and Angles (deg) for Three-Coordinate, Mononuclear Gold Complexes

	$Au(PCy_3)_2Br^a$	$Au(PCy_3)_2Br^a$	$Au(PCy_3)_2Br^a$	$Au(PCy_3)_2Br^a$	
	α	β molecule 1	β molecule 2	γ	$Au(PPh_3)_2Br^b$
bond distances (Å)					
Au1—Br1	3.764(4)	2.894(1)	2.842(1)	2.777(2)	2.625(2)
Au1—P1	2.328(3)	2.317(3)	2.292(3)	2.323(2)	2.323(2)
Au1—P2	2.305(3)	2.311(3)	2.302(3)	2.323(2)	2.323(2)
bond angles (deg)					
P1···Au1···P2	178.4(1)	162.06(9)	157.7(1)	147.5(1)	132.45(8)
P1···Au1···Br1	72.52(9)	99.56(7)	100.51(8)	106.27(6)	113.78(5)
P2···Au1···Br1	109.0(1)	97.69(7)	106.27(6)	106.27(6)	113.78(5)
Σ angles about Au1	359.92	359.31	364.48	357.04	360.34

[a] Data from: Bowmaker, G. A.; Brown, C. L.; Hart, R. D.; Healy, P. C.; Englehardt, L. M.; Rickard, C. E. F.; White, A. H. *J. Chem. Soc., Dalton Trans.* **1999**, 881—889. [b] Data from: Bowmaker, G. A.; Dyason, J. C.; Healy, P. C.; Englehardt, L. M.; Pakawatchai, C.; White, A. H. *J. Chem. Soc., Dalton Trans.* **1987**, 1089—1097.

Structures of the Orange Luminescent Polymers $\{Au(\mu\text{-dppe})Br\}_n \cdot 0.5(C_4H_{10}O)$ and $\{Au(\mu\text{-dppe})Br\}_n \cdot (CH_2Cl_2)$. Type C crystals contain polymeric chains as shown in Figure 5 for $\{Au(\mu\text{-dppe})Br\}_n \cdot (CH_2Cl_2)$. The structure of $\{Au(\mu\text{-dppe})Br\}_n \cdot 0.5(C_4H_{10}O)$ is similar. Within these polymers each gold center is planar and three coordinate with ligation similar to that in crystals of type A and B as the data in Table 2 show. The gold centers are widely separated in these polymers. The closest contact between two gold centers is 7.3645(4) Å for $\{Au(\mu\text{-dppe})Br\}_n \cdot (CH_2Cl_2)$ and 7.1529(7) Å for $\{Au(\mu\text{-dppe})Br\}_n \cdot 0.5(C_4H_{10}O)$. These distances are similar because they are the distances between gold centers within individual chains. The Au···Au separations between the closest gold centers in two adjacent chains are even longer, and clearly there are no aurophilic interactions in these polymers.

Comparisons of Structures within the Three Types of Crystals. The dimeric complexes in crystals of type A and B are all centrosymmetric and share a common ring conformation that is shown in Figure 3. Within these dimers, the coordination geometry of each gold center is planar as shown by the sum of the P—Au—P and P—Au—Br angles given in Table 2. Additionally, the Au—P distances fall in a narrow range (2.3032(6) to 2.3238(14) Å).

However, in other respects the $Au_2(\mu\text{-dppe})_2Br_2$ molecule is remarkably flexible and able to function as a molecular accordion, whose structure depends upon the local crystal environment. Most notably, it is able to accommodate Au1···Au1A separations that range from 3.8479(3) to 3.0943(2) Å. Additionally, the Au—Br distances span a broad range (2.8848(3) to 2.7115(11) Å). The Au—Br distances for the type A crystals are longer (>2.8 Å) than those for the type B crystals, which are less than 2.8 Å. Long Au—Br distances are associated with long Au1···Au1A separations and also with wide P1—Au—P2 angles, which are found to range from 157.89(2) to 139.98(4)° in these dimers. Finally, there are considerable variations in the Br—Au—P angles, which can range from 114.06(4) to 96.582(14)°. Moreover, within a single molecule, the two Br—Au—P angles can differ by as much as 9.1° or as little as 0.5°. While these structural differences are associated with the presence of various solvate molecules in the individual crystals, there do not appear to be readily identifiable interactions such as coordination to gold or hydrogen bonding between the dimer molecules and the solvate molecules. Rather, the solvate molecules occupy space within the crystals, and the dimer seems to alter its geometry to accommodate the space available within a particular crystalline environment.

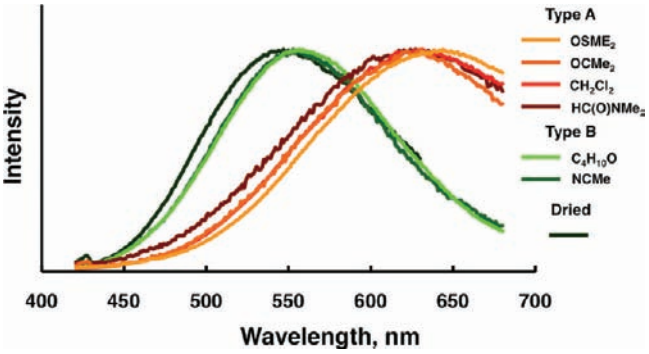

Figure 6. Emission spectra for crystals of type A and B and dried crystals at room temperature.

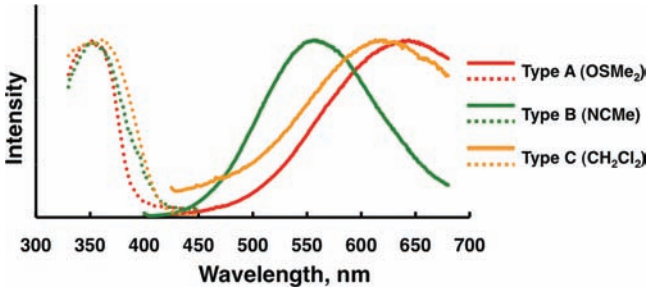

Figure 7. Emission and excitation spectra for representative crystals of types A, B, and C at room temperature.

The bond angles and distances about gold in the polymeric crystals of type C, where the separations between gold centers are quite long, are most similar to those in $Au_2(\mu\text{-dppe})_2Br_2\cdot 2(OSMe_2)$, which is the type A crystal with the longest Au···Au separation.

Variations in the Au—Br distances and P—Au—P angles are common in complexes of the general type, $(R_3P)_2AuBr$, as the data in Table 3 show. The case of $(Cy_3P)_2AuBr$, where Cy = cyclohexyl is particularly interesting.[35] This compound crystallizes in three polymorphic forms (α, β, γ) with the β form containing two molecules in the asymmetric unit. Within the four different molecular structures, the Au—Br distances range from 3.764(4) to 2.777(2) Å, while the P—Au—P angles vary from 178.4(1) to 147.5(1)°. In $(Ph_3P)_2AuBr$, the Au—Br distance, 2.625(2) Å, is even shorter, and the P—Au—P angle is narrower, 132.45(8)°, than any of the corresponding parameters for $(Cy_3P)_2AuBr$.[36]

It is also clear that, despite the variations in the Au—Br distances and in the Br—Au—P and P—Au—P angles, the bromide ions are coordinated in all of these dimeric solvates. The cation, $[Au_2(\mu\text{-dppe})_2]^{2+}$, with two-coordinate gold, has been isolated in crystalline form with poorly coordinating anions. For $[Au_2(\mu\text{-dppe})_2](CF_3SO_3)_2\cdot 2(CH_3CN)$,[37] the P—Au—P angles are nearly linear (177.10 (5), 171.77 (5)°) and the Au···Au separation (2.9220 (3) Å) is much shorter than any of the Au···Au separations reported here for solvates of $Au_2(\mu\text{-dppe})_2Br_2$. Similarly, in $[Au_2(\mu\text{-dppe})_2](PF_6)_2$,[38] the Au···Au separation (2.935 (1) Å) is short, and the P—Au—P angle (160.6(1)°) is bent inward in a fashion that accommodates the short Au···Au distance.

Luminescence and Vapoluminescence. Emission spectra for the various crystals of types A and B are shown in Figure 6. As the figure shows, various crystals of type A produce similar room-temperature emissions with λ_{max} in the range 640—620 nm, while those of type B produce emissions centered at 550 nm. Figure 7 shows emission and excitation spectra for representative crystals of each type. Type A crystals of the dimer and those of the polymer $\{Au(\mu\text{-dppe})Br\}_n\cdot(CH_2Cl_2)$ exhibit similar emission maxima at ca. 620 nm.

Some of the crystals of types A and B exhibit vapoluminescent properties. Thus, upon exposure to air or drying in vacuum, crystals of $Au_2(\mu\text{-dppe})_2Br_2\cdot 2(CH_2Cl_2)$ and $Au_2(\mu\text{-dppe})_2Br_2\cdot 2(OCMe_2)$ of type A lose their orange emission and acquire a green luminescence. Figure 8 shows photographs of crystals of $Au_2(\mu\text{-dppe})_2Br_2\cdot 2(CH_2Cl_2)$ before and after solvate removal by drying in air. While the crystals retain their external morphology, the change in the color of the emission is readily apparent. Exposure of the solvate-free, green glowing crystals to acetone vapor results in their conversion into orange-glowing crystals as shown in parts c and d of Figure 8. The loss of the solvate molecules can be monitored by infrared spectroscopy. For example, after drying in air, crystals of $Au_2(\mu\text{-dppe})_2Br_2\cdot 2(OCMe_2)$ lose the band at 1703vs cm^{-1}, which is $\nu(C{=}O)$ for acetone.

The processes shown in Figure 8 have also been monitored by X-ray powder diffraction as shown in Figure 9. Traces A and B of Figure 9 compare the powder diffraction pattern computed from the single crystal data for $Au_2(\mu\text{-dppe})_2Br_2\cdot 2(OCMe_2)$ with the experimental data obtained from a polycrystalline sample of $Au_2(\mu\text{-dppe})_2Br_2\cdot 2(OCMe_2)$. As shown in trace C of Figure 9, air drying of $Au_2(\mu\text{-dppe})_2Br_2\cdot 2(OCMe_2)$ results in the loss of the characteristic features seen in traces A and B and the development of a new pattern of a second crystalline phase, one that is green glowing when irradiated with near UV light. However, upon exposure to acetone vapor, the powder pattern shown in trace C is replaced by the powder pattern shown in trace D. The data in traces A, B, and D are similar and consistent with the reformation of $Au_2(\mu\text{-dppe})_2Br_2\cdot 2(OCMe_2)$ after exposure to acetone vapor. The new crystalline phase responsible for the green luminescence shown in Figure 8 produces the powder pattern shown in trace C of Figure 9. Unfortunately, efforts to obtain single crystals of this phase have not succeeded. However, based on the data for the green emitting solvates of type B ($Au_2(\mu\text{-dppe})_2Br_2\cdot(NCMe)$ and $Au_2(\mu\text{-dppe})_2Br_2\cdot 0.5(C_4H_{10}O)$) it appears that the new phase responsible for the powder pattern seen in trace C of Figure 9 retains the dimeric structure but possesses a shorter Au···Au separation than that seen in the original, orange luminescent $Au_2(\mu\text{-dppe})_2Br_2\cdot 2(OCMe_2)$.

The green luminescent crystals obtained after drying the type A crystals of $Au_2(\mu\text{-dppe})_2Br_2\cdot 2(CH_2Cl_2)$ and $Au_2(\mu\text{-dppe})_2Br_2\cdot 2(OCMe_2)$ respond to dichloromethane vapor in the same fashion as they do with acetone vapor. However, they do not change their luminescence when exposed to vapors of carbon disulfide, diethyl ether, benzene, acetonitrile, pyridine, nitromethane, dimethyl formamide, or dimethyl sulfoxide. With methanol, the green emitting phase slowly transforms into an orange emitting form. After a two to three hour period partial conversion to the orange emitting form can be visually detected, but about 15 h is required for the complete conversion.

Not all crystals of type A exhibit this sort of behavior. Thus, crystals of $Au_2(\mu\text{-dppe})_2Br_2\cdot 2(OSMe_2)$ and $Au_2(\mu\text{-dppe})_2Br_2\cdot 2(HC(O)NMe_2)$ retain their orange luminescence when exposed to air or dried under vacuum. The volatility of the solvate

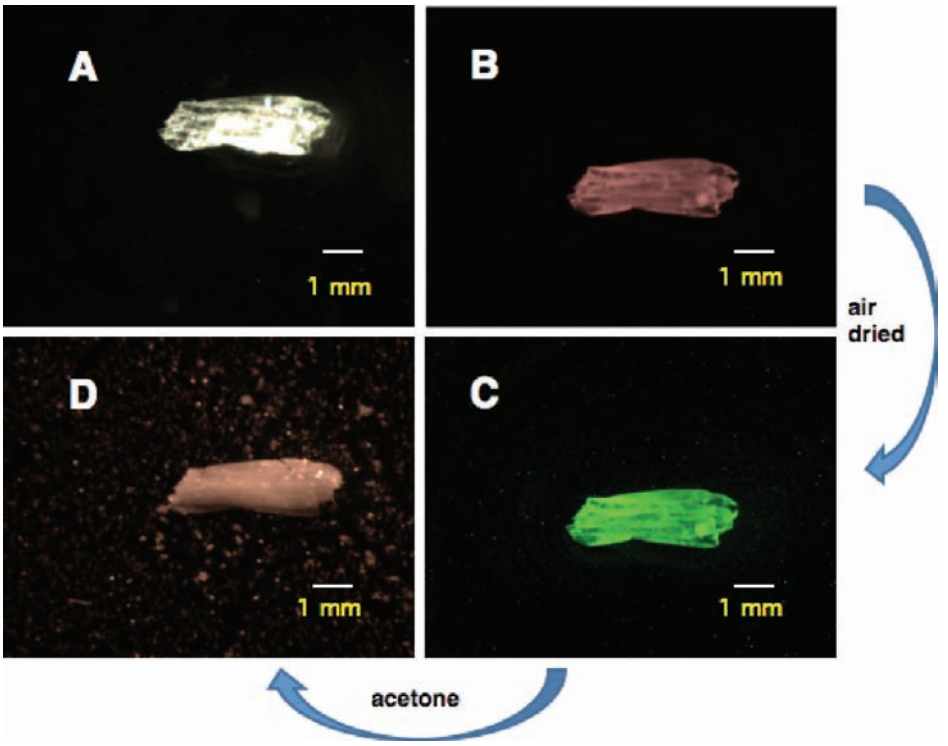

Figure 8. Photographs of crystals of $Au_2(\mu\text{-dppe})_2Br_2\cdot 2(CH_2Cl_2)$: A, under ambient light; B, under UV irradiation; C, under UV irradiation after drying in air; and D, under UV irradiation after exposing the dried crystals to acetone vapor.

molecules appears to determine which crystals of type A undergo the change from orange to green emission. Only those crystals with the most volatile solvate molecules (acetone and dichloromethane) show this transformation.

However, the orange emitting crystals of type C, which involve polymeric strands rather than discrete dimers, do not show any change in emission upon drying. Thus, while crystals of the dimeric complexes, $Au_2(\mu\text{-dppe})_2Br_2\cdot 2(OCMe_2)$ and $Au_2(\mu\text{-dppe})_2Br_2\cdot 2(CH_2Cl_2)$, change their emission from orange to green after standing in air for 10 min, crystals of $\{Au(\mu\text{-dppe})Br\}_n\cdot 0.5(C_4H_{10}O)$ and $Au(\mu\text{-dppe})Br\}_n\cdot(CH_2Cl_2)$ retain their orange luminescence after standing in air for a day. Likewise, crystals of type B do not change their luminescence when exposed to air or vacuum, and they do not show vapoluminescent behavior.

CONCLUSIONS

Our results indicate that crystallization of materials containing the components Au^+, dppe, and Br^- in a 1:1:1 ratio can produce three different types of crystals suitable for analysis by single crystal X-ray diffraction. In one case, all three phases crystallize in the same tube. Orange emitting crystals of type A and green glowing crystals of type B contain the dimer, $Au_2(\mu\text{-dppe})_2Br_2$, while crystals of type C involve a linear polymer as shown in Figure 5. A number of other linear polymers of this type with other bridging diphosphines have been reported previously.[39−41] In all three types of crystals, dppe functions as a bridging ligand. Interestingly, we have not encountered dppe acting as a chelating ligand in any of the complexes we have crystallized. Dppe is, of course, well designed to function as a chelating ligand and does form chelate rings in the four-coordinate cation, $[Au(dppe)_2]^+$.[34]

The orange-luminescent type A crystals of $Au_2(\mu\text{-dppe})_2Br_2\cdot 2(CH_2Cl_2)$ and $Au_2(\mu\text{-dppe})_2Br_2\cdot 2(OCMe_2)$ acquire a green luminescence upon solvate loss but regain the orange luminescence upon exposure to vapors of acetone or dichloromethane. This is a selective process. Vapors of carbon disulfide, diethyl ether, benzene, acetonitrile, pyridine, nitromethane, dimethyl formamide, or dimethyl sulfoxide do not restore the orange luminescence. The marked flexibility of the $Au_2(\mu\text{-dppe})_2Br_2$ molecule is intimately associated with the variations in luminescence and the vapoluminescent behavior shown in Figures 1 and 6−8. The approach of the two gold centers seen in the crystals of type B results in greater overlap of the out-of-plane p_z orbitals and a corresponding diminution in the HOMO−LUMO gap. As a result, the excitation profile for crystals of type B shows a low-energy shoulder at ca. 400 nm that is not present in the excitation spectrum of the crystals of type A. The difference in luminescence between the crystals of type A and B can be ascribed largely to a difference in the Stokes' shifts for the two types with the green emitting crystals having a lesser Stokes' shift. The fact that the orange emitting crystalline polymers of type C polymers do not display variations in luminescence is consistent with the fact that these polymers do not contain the flexible $Au_2(\mu\text{-dppe})_2Br_2$ molecule. To obtain that molecule from the polymer, considerable bond breaking and remaking would have to occur, a situation that is unlikely to occur in the solid state.

Finally, it is important to note that the present compounds present the first evidence for the significance of aurophilic interactions between three-coordinate gold(I) centers where close contacts between the gold centers are not enforced by small-bite bridging ligands, as is the case with $[Au_2(\mu\text{-dmpm})_3](BF_4)_2$ and related compounds mentioned in the Introduction.[20]

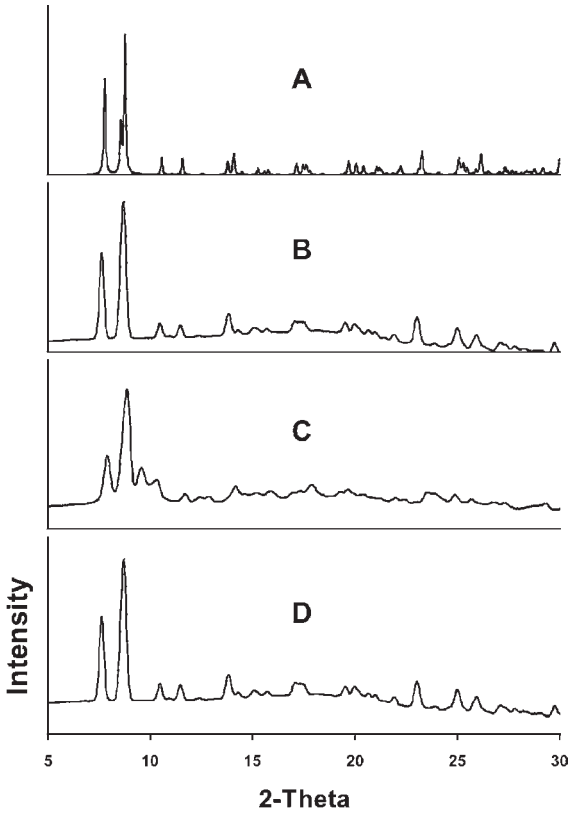

Figure 9. Powder X-ray diffraction data for orange luminescent $Au_2(\mu\text{-dppe})_2Br_2\cdot 2(OCMe_2)$: A, calculated pattern from the single crystal data; B, experimental powder data; C, dried sample from B with green luminescence; D, orange luminescent sample obtained after exposing sample shown in C to acetone vapor.

EXPERIMENTAL SECTION

Materials. A previously reported procedure was used for the preparation of (tht)AuBr (tht = tetrahydrothiophene).[42]

Preparation of Au(dppe)Br. A 100 mg (0.274 mmol) portion of (tht)AuBr was dissolved in 30 mL of dichloromethane. While stirring, 164 mg (0.412 mmol) of dppe was added. After stirring for 2 h, the solution was filtered, and then the solvent was removed in a vacuum. The white solid with green luminescence was collected and washed with diethyl ether: yield, 160 mg (86.5%). This material was used to obtain crystalline samples of the following compounds.

$Au_2(\mu\text{-dppe})_2Br_2\cdot 2(OSMe_2)$. The original white solid was dissolved in a minimum volume of dimethyl sulfoxide, and the colorless solution was filtered. After evaporation for a week, colorless blocks with an orange luminescence grew from the solution. These were used for the X-ray diffraction and spectral studies. Infrared spectrum: 3047w, 3005w, 2892w, 1484s, 1432s, 1406m, 1315m, 1100w, 1013s, 950m, 746m, 705m, 690s, 522m, 509m, 485m cm^{-1}.

$Au_2(\mu\text{-dppe})_2Br_2\cdot 2(CH_2Cl_2)$ and $\{Au(\mu\text{-dppe})Br\}_n\cdot(CH_2Cl_2)$. The suitable crystals for X-ray structure determination were grown by slow diffusion of diethyl ether to a saturated solution of the initial white solid in dichloromethane. The colorless blocks of $Au_2(\mu\text{-dppe})_2Br_2\cdot 2(CH_2Cl_2)$ with an orange luminescence formed over a one day period in the dichloromethane-rich layer at the bottom of the tube. Simultaneously, another set of colorless blocks appeared in the diethyl ether-rich layer at the upper part of the tube. These orange luminescent crystals were identified as the polymer, $\{Au(\mu\text{-dppe})Br\}_n\cdot(CH_2Cl_2)$. Infrared spectrum $Au_2(\mu\text{-dppe})_2Br_2\cdot 2(CH_2Cl_2)$: 3048w, 3006w, 2891w, 1480m, 1433s, 1413m, 1307w, 1265w, 1179w, 1157w, 1100s, 1069m, 1026w, 997w, 917w, 879w, 819w, 744m, 724s, 707m, 689vs, 521m, 508s, 475m cm^{-1}. Infrared spectrum polymeric $\{Au(\mu\text{-dppe})Br\}_n\cdot(CH_2Cl_2)$: 3047w, 2973w, 2895w, 1479s, 1433s, 1412m, 1311m, 1098s, 1073m, 950m, 750m, 726s, 688s, 522m, 508s, 487m, 478m cm^{-1}.

$Au_2(\mu\text{-dppe})_2Br_2\cdot 2(HC(O)NMe_2)$. The white solid was dissolved in a minimum volume of *N,N*-dimethylformamide, and the colorless solution was filtered. After evaporation for a week, colorless blocks grew in the solution. These crystals, which produced an orange luminescence, were used for the spectroscopy and crystallography. Infrared spectrum: 3049w, 3008w, 2895w, 1658s (νC=O from $HC(O)NMe_2$), 1484m, 1432s, 1414m, 1379m, 1098s, 822m, 740w, 715s, 689s, 659m, 523m, 510s, 490m, 475m cm^{-1}.

$Au_2(\mu\text{-dppe})_2Br_2\cdot(NCMe)$. The white solid was dissolved in a minimum volume of acetonitrile, and the solution was filtered. After an hour, the colorless plates with a green luminescence grew in the solution. These crystals were utilized in the spectroscopic and crystallographic studies. Infrared spectrum: 3049w, 3008w, 2893w, 2251w (νC≡N from acetonitrile), 1481m, 1432s, 1412m, 1100s, 825m, 745m, 688s, 523m, 508s, 483m, 475m cm^{-1}.

$Au_2(\mu\text{-dppe})_2Br_2\cdot 2(OCMe_2)$, $Au_2(\mu\text{-dppe})_2Br_2\cdot 0.5(C_4H_{10}O)$, and $\{Au(\mu\text{-dppe})Br\}_n\cdot 0.5(C^4H_{10}O)$. Colorless (tht)AuBr (100 mg, 0.274 mmol) was dissolved in 30 mL of acetone. While stirring, solid dppe (164 mg, 0.412 mmol) was added. After additional stirring for 2 h, the solution was filtered, and then the solvent was removed in a vacuum. The white solid was collected and washed with diethyl ether. The yield was 155 mg (84.3%). Crystals suitable for X-ray structure determination were grown by slow diffusion of diethyl ether to a solution of the colorless solid in acetone. Colorless, orange emitting crystals of $Au_2(\mu\text{-dppe})_2Br_2\cdot 2(OCMe_2)$ appeared near the bottom of the tube in the acetone-rich section. Colorless, orange luminescent crystals of $\{Au(\mu\text{-dppe})Br\}_n\cdot 0.5(C_4H_{10}O)$ appeared in the upper, diethyl ether-rich portion of the tube. Additionally, but not in every case, colorless, green luminescent crystals of $Au_2(\mu\text{-dppe})_2Br_2\cdot 0.5(C_4H_{10}O)$ also appeared in a separate region in the upper, diethyl ether-rich portion of the tube. Infrared spectrum for $Au_2(\mu\text{-dppe})_2Br_2\cdot 2(OCMe_2)$: 3047w, 3003w, 2905w, 1703vs (ν(C=O) from acetone), 1584m, 1481m, 1432vs, 1410m, 1358m, 1309m, 1275m, 1221m, 1095m, 1070m, 1025m, 997m, 87m1, 833m, 809m, 738s, 689vs, 661m, 642w, 616w, 556w, 519m, 508s, 475m cm^{-1}. Infrared spectrum for $Au_2(\mu\text{-dppe})_2Br_2\cdot 0.5(C_4H_{10}O)$: 3045w, 3007w, 2892w, 1480m, 1433s, 1411m, 1309w, 1124m, 1100s, 1069m, 998w, 826m, 748s, 689s, 524m, 508s, 485m, 470m cm^{-1}. Infrared spectrum for $\{Au(\mu\text{-dppe})Br\}_n\cdot 0.5(C_4H_{10}O)$: 3048w, 2975w, 2896w, 1481s, 1432s, 1412m, 1315m, 1100s, 1073m, 950m, 750m, 726s, 690s, 521m, 511s, 487m, 475m cm^{-1}.

X-ray Crystallography and Data Collection. The crystals were removed from the glass tubes in which they were grown together with a small amount of mother liquor and immediately coated with a hydrocarbon oil on a microscope slide. A suitable crystal of each compound was mounted on a glass fiber with silicone grease and placed in the cold stream of a Bruker SMART CCD with graphite monochromated Mo Kα radiation at 90(2) K.

The structures were solved by direct methods and refined using all data (based on F^2) using the software SHELXTL 5.1. A semiempirical method utilizing equivalents was employed to correct for absorptions. Hydrogen atoms were added geometrically and refined with a riding model.[43]

Physical Measurements. Infrared spectra were recorded on a Bruker ALPHA FT-IR spectrometer. Fluorescence excitation and emission spectra were recorded on a Perkin-Elmer LS50B luminescence spectrophotometer.

ASSOCIATED CONTENT

Supporting Information. Drawings of the molecular structures from all of the crystals. X-ray crystallographic files in CIF

format for $Au_2(\mu\text{-dppe})_2Br_2\cdot 2(OSMe_2)$, $Au_2(\mu\text{-dppe})_2Br_2\cdot 2(OCMe_2)$, $Au_2(\mu\text{-dppe})_2Br_2\cdot 2(CH_2Cl_2)$, $Au_2(\mu\text{-dppe})_2Br_2\cdot 2(HC(O)NMe_2)$, $Au_2(\mu\text{-dppe})_2Br_2\cdot(NCMe)$, $Au_2(\mu\text{-dppe})_2Br_2\cdot 0.5(C_4H_{10}O)$, $\{Au(\mu\text{-dppe})Br\}_n\cdot 0.5(C_4H_{10}O)$, and $\{Au(\mu\text{-dppe})Br\}_n\cdot(CH_2Cl_2)$. This material is available free of charge via the Internet at http://pubs.acs.org.

AUTHOR INFORMATION

Corresponding Author
albalch@ucdavis.edu

ACKNOWLEDGMENT

We thank the Petroleum Research Fund (Grant 37056-AC to ALB) and U.S. National Science Foundation [CHE-0716843 and CHE-1011760 to ALB and MMO] for support and Dr. D. Rios for experimental assistance.

REFERENCES

(1) Fiddler, M. N.; Begashaw, I.; Mickens, M. A.; Collingwood, M. S.; Assefa, Z.; Bililign, S. *Sensors* **2009**, *9*, 10447–10512.
(2) Elosúa, C.; Bariain, C.; Matias, I. R.; Arregui, F. J.; Vergara, E.; Laguna, M. *Sens. Actuators, B* **2009**, *137*, 139–146.
(3) (a) Drew, S. M.; Janzen, D. E.; Buss, C. E.; MacEwan, D. I.; Dublin, K. M.; Mann, K. R. *J. Am. Chem. Soc.* **2001**, *123*, 8414–8415. (b) Drew, S. M.; Janzen, D. E.; Mann, K. R. *Anal. Chem.* **2002**, *74*, 2547–2555.
(4) Pyykkö, P. *Chem. Rev.* **1997**, *97*, 597–636.
(5) Pyykkö, P. *Angew. Chem., Int. Ed.* **2004**, *43*, 4412–4456.
(6) Fernández, E. J.; López-de-Luzuriaga, J. M.; Monge, M.; Olmos, M. E.; Javier Pérez, J.; Laguna, A.; Mohamed, A. A.; Fackler, J. P., Jr. *J. Am. Chem. Soc.* **2003**, *125*, 2022–2023.
(7) Strasser, C. E.; Catalano, V. J. *J. Am. Chem. Soc.* **2010**, *132*, 10009–10011.
(8) Fernández, E. J.; López-de-Luzuriaga, J. M.; Monge, M.; Olmos, M. E.; Puelles, R. C.; Laguna, A.; Mohamed, A. A.; Fackler, J. P., Jr. *Inorg. Chem.* **2008**, *47*, 8069–8076.
(9) Ley, A. N.; Dunaway, L. E.; Timothy P. Brewster, T. P.; Dembo, M. D.; Harris, T. D.; Baril-Robert, F.; Li, X.; Patterson, H. H.; Pike, R. D. *Chem. Commun.* **2010**, *46*, 4565–4567.
(10) Buss, C. E.; Anderson, C. E.; Pomije, M. K.; Lutz, C. M.; Britton, D.; Mann, K. R. *J. Am. Chem. Soc.* **1998**, *120*, 7783–7790.
(11) Daws, C. A.; Exstrom, C. L.; Sowa, J. R., Jr.; Mann, K. R. *Chem. Mater.* **1997**, *9*, 363–368.
(12) Wadas, T. J.; Wang, Q.-M.; Kim, Y.; Flaschenreim, C.; Blanton, T. N.; Eisenberg, R. *J. Am. Chem. Soc.* **2004**, *126*, 16841–16849.
(13) Exstrom, C. L.; Pomije, M. K.; Mann, K. R. *Chem. Mater.* **1998**, *10*, 942–945.
(14) Balch, A. L. *Struct. Bonding (Berlin)* **2007**, *123*, 1–40.
(15) Yam, V. W. W.; Chung-Chin Cheng, E. C. C. *Chem. Soc. Rev.* **2008**, *37*, 1806–1813.
(16) Pyykkö, P. *Chem. Soc. Rev.* **2008**, *37*, 1967–1997.
(17) Pathaneni, S. S.; Desiraju, G. R. *J. Chem. Soc., Dalton Trans.* **1993**, 319–322.
(18) Anderson, K. A.; Goeta, A. E.; Steed, J. W. *Inorg. Chem.* **2007**, *46*, 6444–6451.
(19) Schmidbaur, H.; Schier, A. *Chem. Soc. Rev.* **2008**, *37*, 1931–1951.
(20) Bensch, W.; Prelati, M.; Ludwig, W. *Chem. Commun.* **1986**, 1762–1763.
(21) Bojan, V. R.; Ferández, E. J.; Laguna, A.; López-de-Luzuriaga, J. M.; Monge, M.; Olmos, M. E.; Silvestru, C. *J. Am. Chem. Soc.* **2005**, *127*, 11564–11565.
(22) Shain, J.; Fackler, J. P., Jr. *Inorg. Chim. Acta* **1987**, *131*, 157–158.
(23) Xiao, H.; Weng, Y.-X.; Wong, W.-T.; Mak, T. C. W.; Che, C. M. *Dalton Trans.* **1997**, 221–226.
(24) Schmidbaur, H.; Herr, R.; Muller, G.; Riedet, J. *Organometallics* **1985**, *4*, 1208–1213.
(25) Schmidbaur, H.; Pollok, Th.; Herr, R.; Wagner, F. E.; Bau, R.; Riede, J.; Müller, G. *Organometallics* **1986**, *5*, 566–574.
(26) Ziolo, R.; Lipton, S.; Z. Dori, Z. *Chem. Commun.* **1970**, 1124–1125.
(27) McCleskey, T. M.; Gray, H. B. *Inorg. Chem.* **1992**, *31*, 1773–1734.
(28) King, C.; Khan, M. N. I.; Staples, R. J.; Fackler, J. P., Jr. *Inorg. Chem.* **1992**, *31*, 3236–3238.
(29) Barakat, K. A.; Cundari, T. R.; Omary, M. A. *J. Am. Chem. Soc.* **2003**, *125*, 14228–14229.
(30) Sinha, P.; Wilson, A. K.; Omary, M. A. *J. Am. Chem. Soc.* **2005**, *127*, 12488–12489.
(31) Hoshino, M; Uekusa, H; Ohashi, Y. *Bull. Chem. Soc. Jpn.* **2006**, *79*, 1362–1366.
(32) Hoshino, M.; Uekusa, H.; Sonoda, S.; Takuhiro Otsuka, T.; Kaizu, Y. *Dalton Trans.* **2009**, 3085–3091.
(33) Hoshino, M.; Uekusa, H.; Ishii, S.; Otsuka, T.; Kaizu, Y.; Ozawa, Y.; Toriumi, K. *Inorg. Chem.* **2010**, *49*, 7257–7265.
(34) Berners-Price, S. J.; Mazid, M. A.; Sadler, P. J. *J. Chem. Soc., Dalton Trans.* **1984**, 969–974.
(35) Bowmaker, G. A.; Brown, C. L.; Hart, R. D.; Healy, P. C.; Englehardt, L. M.; Rickard, C. E. F.; White, A. H. *J. Chem. Soc., Dalton Trans.* **1999**, 881–889.
(36) Bowmaker, G. A.; Dyason, J. C.; Healy, P. C.; Englehardt, L. M.; Pakawatchai, C.; White, A. H. *J. Chem. Soc., Dalton Trans.* **1987**, 1089–1097.
(37) Strasser, C. E.; Cronje, S.; Raubenheimer, H. G. *Acta Crystallogr., Sect. E: Struct. Rep. Online* **2009**, *E65*, m914.
(38) Schaefer, W. P.; Marsh, R. E.; McCleskey, T. M.; Gray, H. B. *Acta Crystallogr., Sect. C: Cryst. Struct. Commun* **1991**, *47*, 2553–2556.
(39) Brandys, M.-C.; Puddephatt, R. J. *Chem. Commun.* **2001**, 1280–1281.
(40) Brandys, M.-C.; Puddephatt, R. J. *J. Am. Chem. Soc.* **2001**, *123*, 4839–4840.
(41) Puddephatt, R. J. *Chem. Soc. Rev.* **2008**, *37*, 2012–2027.
(42) Uson, R.; Laguna, A.; Laguna, M. *Inorg. Synth.* **1989**, *26*, 85.
(43) Sheldrick, G. M. *Acta Crystallogr., Sect. A* **2008**, *64*, 112–122.